

Hydrogelation and Self-Assembly of Fmoc-Tripeptides: Unexpected Influence of Sequence on Self-Assembled Fibril Structure, and Hydrogel Modulus and Anisotropy

G. Cheng, V. Castelletto, C. M. Moulton, G. E. Newby, and I. W. Hamley*

Department of Chemistry, University of Reading, Reading RG6 6AD, United Kingdom

Received September 29, 2009. Revised Manuscript Received December 1, 2009

The self-assembly and hydrogelation properties of two Fmoc-tripeptides [Fmoc = *N*-(fluorenyl-9-methoxycarbonyl)] are investigated, in borate buffer and other basic solutions. A remarkable difference in self-assembly properties is observed comparing Fmoc-VLK(Boc) with Fmoc-K(Boc)LV, both containing K protected by *N*^ε-*tert*-butyloxycarbonate (Boc). In borate buffer, the former peptide forms highly anisotropic fibrils which show local alignment, and the hydrogels show flow-aligning properties. In contrast, Fmoc-K(Boc)LV forms highly branched fibrils that produce isotropic hydrogels with a much higher modulus ($G' > 10^4$ Pa), and lower concentration for hydrogel formation. The distinct self-assembled structures are ascribed to conformational differences, as revealed by secondary structure probes (CD, FTIR, Raman spectroscopy) and X-ray diffraction. Fmoc-VLK(Boc) forms well-defined β -sheets with a cross- β X-ray diffraction pattern, whereas Fmoc-KLV(Boc) forms unoriented assemblies with multiple stacked sheets. Interchange of the K and V residues when inverting the tripeptide sequence thus leads to substantial differences in self-assembled structures, suggesting a promising approach to control hydrogel properties.

Introduction

Short peptides are attracting great interest as low molecular weight gelators, in particular hydrogelators.^{1,2} Molecules such as dipeptide derivatives are attractive for the development of novel biomaterials, and have been demonstrated to be usable as scaffolds for cell growth with potential applications in tissue engineering.^{1,3–6}

The self-assembly and hydrogelation of Fmoc-dipeptides [Fmoc = *N*-(fluorenyl-9-methoxycarbonyl)] and dipeptides conjugated to other bulky aromatic units such as naphthalene have been investigated in detail by the groups of Xu,^{7,8} Ulijn,^{2,4–6,9} Gazit,¹⁰ and others.¹¹ Even Fmoc-amino acids such as Fmoc-phenylalanine or Fmoc-tyrosine are able to form hydrogels in appropriate acidic media.¹² Responsive materials have been developed that undergo sol–gel transitions in response to ligand

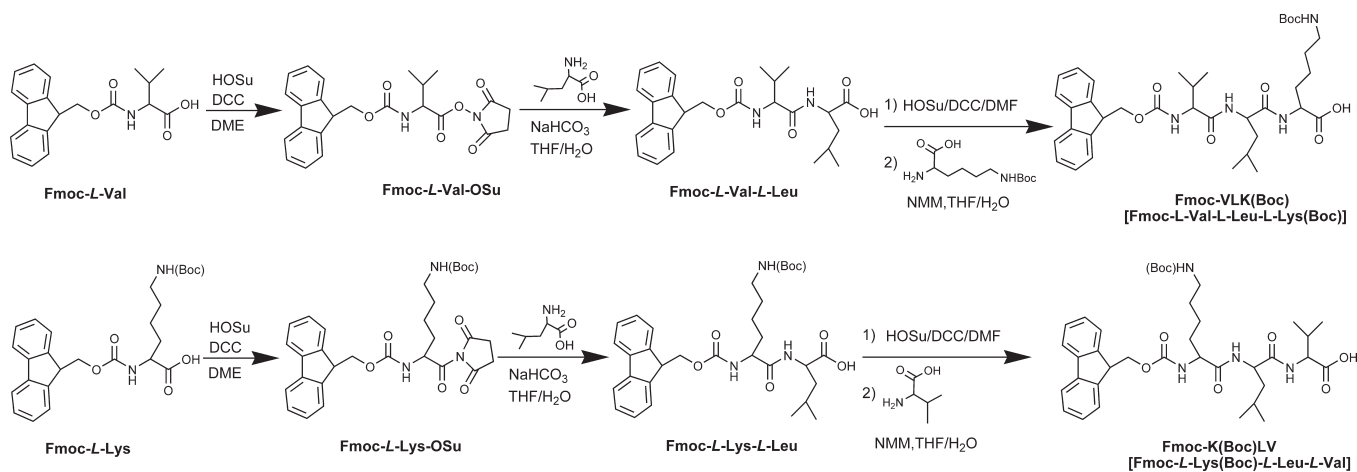
(vancomycin) binding.¹³ Fmoc-dipeptides containing non-natural residues have recently been investigated by the Xu group due to their enhanced biostability, that is, potential for use in controlled drug release.¹⁴ Enzyme-catalyzed formation of hydrogels based on Fmoc-peptides has been reported.^{9,15} The formation of hydrogels from other short peptides with bulky aromatic end units (e.g., naphthalene) in response to enzyme has recently been investigated. The peptide was a tripeptide comprising a sequence of two β -amino acids (providing enhanced biostability) and an α -amino acid (tyrosine phosphate), responsive to a phosphatase enzyme.¹⁶ An assay for enzyme inhibitors based on a smaller Fmoc-amino acid (Fmoc-tyrosine phosphate) was also reported, relying on hydrogelation.^{7,17} The hydrogels formed by the Fmoc-peptides studied by Xu and co-workers are based on superhelical arrangements of the aromatic residues, possibly driven by π – π * stacking interactions.^{8,15} Ulijn and co-workers have, in a similar vein, investigated the enzymatic hydrogelation and dehydrogelation of Fmoc-dipeptides using subtilisin to hydrolyze C-terminal esters and thermolysin to induce reverse hydrolysis (linking an Fmoc-amino acid with amino acid methyl esters).¹⁸

There are few studies on Fmoc-tripeptides. Ulijn and co-workers prepared tripeptides Fmoc-*X*-F₂ (*X* = G, A, V, F, P, L) by reverse hydrolysis,⁹ using thermolysin as described above. Banerjee and co-workers have investigated the self-assembly into fibrils¹⁹ or nanotubes²⁰ of certain non-Fmoc-tripeptides and have examined organogelation of peptides protected at the N terminus

*To whom correspondence should be addressed. E-mail: I.W.Hamley@reading.ac.uk. Also at Diamond Light Source, Harwell Science and Innovation Campus, Didcot OX11 0DE, U.K.

(1) Xu, B. *Langmuir* **2009**, *25*(15), 8375–8377.
(2) Mart, R. J.; Osborne, R. D.; Stevens, M. M.; Ulijn, R. V. *Soft Matter* **2006**, *2*, 822–835.
(3) Yang, Z.; Xu, K.; Wang, L.; Gu, H.; Wei, H.; Zhang, M.; Xu, B. *Chem. Commun.* **2005**, 4414–4416.
(4) Zhou, M.; Smith, A. M.; Das, A. K.; Hodson, N. W.; Collins, R. F.; Ulijn, R. V.; Gough, J. E. *Biomaterials* **2009**, *30*(13), 2523–2530.
(5) Jayawarna, V.; Ali, M.; Jowitt, T. A.; Miller, A. F.; Saiani, A.; Gough, J. E.; Ulijn, R. V. *Adv. Mater.* **2006**, *18*, 611–614.
(6) Jayawarna, V.; Richardson, S. M.; Hirst, A. R.; Hodson, N. W.; Saiani, A.; Gough, J. E.; Ulijn, R. V. *Acta Biomater.* **2009**, *5*(3), 934–943.
(7) Yang, Z.; Xu, B. *Chem. Commun.* **2004**, 2424–2425.
(8) Yang, Z.; Liang, G.; Ma, M.; Gao, Y.; Xu, B. *J. Mater. Chem.* **2007**, *17*, 850–854.
(9) Toledano, S.; Williams, R. J.; Jayawarna, V.; Ulijn, R. V. *J. Am. Chem. Soc.* **2006**, *128*(4), 1070–1071.
(10) Mahler, A.; Reches, M.; Rechter, M.; Cohen, S.; Gazit, E. *Adv. Mater.* **2006**, *18*, 1365–1370.
(11) Adams, D. J.; Butler, M. F.; Frith, W. J.; Kirkland, M.; Mullen, L.; Sanderson, P. *Soft Matter* **2009**, *5*(9), 1856–1862.
(12) Sutton, S.; Campbell, N. L.; Cooper, A. I.; Kirkland, M.; Frith, W. J.; Adams, D. J. *Langmuir* **2009**, *25*(17), 10285–10291.
(13) Zhang, Y.; Gu, H.; Yang, Z.; Xu, B. *J. Am. Chem. Soc.* **2003**, *125*, 13680–13681.

(14) Liang, G.; Yang, Z.; Zhang, R.; Li, L.; Fan, Y.; Kuang, Y.; Gao, Y.; Wang, T.; Lu, W. W.; Xu, B. *Langmuir* **2009**, *25*(15), 8419–8422.
(15) Yang, Z.; Gu, H.; Fu, D.; Gao, P.; Lam, J. K. W.; Xu, B. *Adv. Mater.* **2004**, *16*(16), 1440–1444.
(16) Yang, Z.; Liang, G.; Ma, M.; Gao, Y.; Xu, B. *Small* **2007**, *3*(4), 558–562.
(17) Yang, Z.; Xu, B. *Adv. Mater.* **2006**, *18*, 3043–3046.
(18) Das, A. K.; Collins, R.; Ulijn, R. V. *Small* **2008**, *2*, 279–287.
(19) Naskar, J.; Drew, M. G. B.; Deb, I.; Das, S.; Banerjee, A. *Org. Lett.* **2008**, *10*(13), 2625–2628.
(20) Ray, S.; Haldar, D.; Drew, M. G. B.; Banerjee, A. *Org. Lett.* **2004**, *6*, 4463–4465.

Scheme 1. Synthesis of Fmoc-Tripeptides Fmoc-VLK (N^t -Boc) and Fmoc-K(N^t -Boc)LV

with aromatic units such as N^t -tert-butyloxycarbonate (Boc) or carbobenzyloxy (Cbz) units.²¹ We have recently been investigating the self-assembly and hydrogelation of peptides containing sequences from the amyloid β ($A\beta$) peptide core sequence $A\beta$ -(16–20), i.e. KLVFF.^{22–24} These sequences do not contain an Fmoc terminus. Without the Fmoc terminus, previous work suggests that KLVFF is the shortest peptide based on a sequence from this region of $A\beta$ capable of self-assembling into β -sheets and forming hydrogels.^{24–26} The dipeptide FF (within KLVFF) can self-assemble into nanotubes in water,^{27,28} but the structure within the walls of these is not based on a β -sheet motif.²⁹ We have been interested to investigate whether the self-assembly of shorter sequences can be induced by attachment to Fmoc which leads to aromatic stacking interactions that can drive fibrillization.¹⁰ The present Article describes our initial studies in this direction. We report on the self-assembly and hydrogelation of Fmoc-K(Boc)LV, which contains the KLV sequence, part of KLVFF, as studied previously by our group and others. The self-assembly and hydrogelation of Fmoc-K(Boc)LV is compared to that of a peptide containing the inverse sequence, Fmoc-VLK(Boc), that is, one in which K(Boc) and V residues are interchanged. For convenience, in the following, the samples are denoted Fmoc-K(Boc)LV and Fmoc-VLK(Boc). The Boc group is retained in order to investigate the role of hydrophobic versus electrostatic interactions; in future work, we will present our ongoing studies on Fmoc-K(Boc)LV and Fmoc-VLK(Boc) with deprotected K groups, and also Fmoc protected K groups. Here, we present a comprehensive study on self-assembly comparing the two Fmoc-tripeptides, studying fibril formation via cryo-transmission electron microscopy (cryo-TEM) and small-angle X-ray scattering (SAXS). The secondary structure is probed via X-ray diffraction, circular dichroism (CD), Fourier transform infrared (FTIR) and Raman spectroscopy. Gel properties are probed via SAXS and

reometry. An unexpected difference in gel dynamic mechanical and structural properties is revealed. In borate buffer, Fmoc-VLK(Boc) exhibits nematic-like ordering of highly anisotropic and aligned fibrils, whereas Fmoc-K(Boc)LV shows a dense branched fibrillar network structure which produces isotropic hydrogels with high rigidity. These gels have numerous potential applications in nanobiotechnology, such as cell growth media, controlled release drug delivery media, enzyme responsive systems, and antimicrobial gels.

Experimental Section

Materials. Amino acids [Fmoc-lysine(Boc)-OH, Fmoc-leucine-OH, Fmoc-valine-OH, Fmoc-phenylalanine-OH], HOBt (1-hydroxybenzotriazole), and HBTU [2-(1H-benzotriazol-1-yl)-1,1,3,3-tetramethyluronium hexafluorophosphate] were purchased from Novabiochem (United Kingdom). *N*-Hydroxysuccinimide (HOSu), 1,3-dicyclohexylcarbodiimide (DCC), *N*-methylmorpholine (NMM), anhydrous dimethoxyethane (DME), anhydrous *N,N*-dimethylformamide (DMF), glucono- δ -lactone (GdL), Congo Red, and citric acid were purchased from Sigma-Aldrich (United Kingdom); sodium bicarbonate, tetrahydrofuran (THF), ethyl acetate (EtOAc), and borate buffer (pH = 10) were purchased from Fisher Scientific (United Kingdom). Scheme 1 describes the route to synthesize Fmoc-tripeptides Fmoc-VLK(Boc) and Fmoc-K(Boc)LV.

Synthesis of Fmoc-L-Val-OSu. *N*-(Fluorenyl-9-methoxycarbonyl) L-Val (5.09 g, 15 mmol) and *N*-hydroxysuccinimide (1.73 g, 15.00 mmol) were dissolved in 80 mL of anhydrous dimethoxyethane. The solution was cooled in ice-water, and a solution of DCC (3.40 g, 16.50 mmol) in 20 mL of anhydrous dimethoxyethane was dropwise added to the solution which became cloudy white. The mixture was stirred for 24 h at room temperature. The urea precipitate was filtered out, and the filtrate was dried by evaporation of the solvent. The resulting product was redissolved in a minimal amount of acetone and then kept in a fridge for 4 h. The small amount of urea precipitate was filtered out, and the filtrate was concentrated to dryness by evaporation of the solvent. The white foam was dissolved in EtOAc and precipitated in petroleum ether (40–60 °C) to give a white powder (6.10 g, 93%). ¹H NMR (250 MHz, DMSO- d_6) δ (ppm): 8.18 (d, J = 10.0 Hz, 1H), 7.92 (d, J = 7.5 Hz, 2H), 7.74 (t, J = 7.5 Hz, 2H), 7.42 (t, J = 7.5 Hz, 2H), 7.33 (t, J = 7.5 Hz, 2H), 4.33 (m, 4H), 2.82 (s, 4H), 2.09 (m, 1H), 1.01 (d, J = 7.5 Hz, 6H).

Synthesis of Fmoc-L-Val-L-Leu. *N*-(Fluorenyl-9-methoxycarbonyl) L-Leu (1.69 g, 12.91 mmol) was dissolved in 200 mL of cosolvent of THF/water (1:1) containing sodium bicarbonate (2.17 g, 25.82 mmol). To this solution, a solution of Fmoc-L-Val-OSu (5.63 g, 12.91 mmol) in 20 mL of acetone was added

(21) Das, A. K.; Bose, P. P.; Drew, M. G. B.; Banerjee, A. *Tetrahedron* **2007**, *63* (31), 7432–7442.

(22) Krysmann, M. J.; Castelletto, V.; Kellarakis, A.; Hamley, I. W.; Hule, R. A.; Pochan, D. J. *Biochemistry* **2008**, *47*, 4597–4605.

(23) Castelletto, V.; Hamley, I. W.; Harris, P. J. F. *Biophys. Chem.* **2008**, *139*, 29–35.

(24) Castelletto, V.; Hamley, I. W.; Hule, R. A.; Pochan, D. J. *Angew. Chem., Int. Ed. Engl.* **2009**, *48*, 2317–2320.

(25) Tjernberg, L. O.; Callaway, D. J. E.; Tjernberg, A.; Hahne, S.; Liljehöök, C.; Terenius, L.; Thyberg, J.; Nordstedt, C. *J. Biol. Chem.* **1999**, *274*(18), 12619–12625.

(26) Gordon, D. J.; Tappe, R.; Meredith, S. C. *J. Pept. Res.* **2002**, *60*, 37–55.

(27) Reches, M.; Gazit, E. *Science* **2003**, *300*, 625–627.

(28) Reches, M.; Gazit, E. *Isr. J. Chem.* **2005**, *45*, 363–371.

(29) Görbitz, C. H. *Chem. Commun.* **2006**, 2332–2334.

dropwise at room temperature. After addition, it was stirred for 48 h and the solvent was concentrated to dryness in vacuo. The crude product was dissolved in 200 mL of EtOAc, washed with 10% aq citric acid and water, and then dried (MgSO₄). It was filtered, and the filtrate was concentrated to dryness in vacuo to give a white powder 4.44 g (76%). ¹H NMR (250 MHz, DMSO-*d*₆) δ (ppm): 8.13 (d, *J* = 7.5 Hz, 1H), 7.90 (d, *J* = 7.5 Hz, 2H), 7.74 (m, 3H), 7.44 (m, 2H), 7.32 (t, *J* = 7.5 Hz, 2H), 4.33–4.12 (m, 4H), 3.91 (m, 1H), 2.02 (m, 1H), 1.68–1.40 (m, 3H), 0.88 (m, 12H). MS: calcd [M⁺] = 452, obsvd [M+1⁺] = 453.

Synthesis of Fmoc-L-Val-L-Leu-L-Lys(Boc). Fmoc-L-Val-L-Leu (4.00 g, 8.84 mmol) and *N*-hydroxysuccinimide (1.02 g, 8.84 mmol) were dissolved in 40 mL of anhydrous dimethoxyethane. The solution was cooled in ice-water, and a solution of DCC (2.00 g, 9.72 mmol) in 10 mL of anhydrous dimethoxyethane was added dropwise to the solution which became cloudy white. The mixture was stirred for 24 h at room temperature. The urea precipitate was filtered out, and the filtrate was concentrated to dryness by evaporation of the solvent. The resulting product was redissolved in a minimal amount of acetone and then kept in a fridge for 4 h. The small amount of urea precipitate was filtered out, and the filtrate was concentrated to dryness by evaporation of the solvent to give white powder Fmoc-L-Val-L-Leu-OSu. ¹H NMR (250 MHz, DMSO-*d*₆) δ (ppm): 8.65 (d, *J* = 7.5 Hz, 1H), 7.91 (d, *J* = 7.5 Hz, 2H), 7.74 (d, *J* = 7.5 Hz, 2H), 7.51 (d, *J* = 7.5 Hz, 1H), 7.42 (t, *J* = 7.5 Hz, 2H), 7.32 (t, *J* = 7.5 Hz, 2H), 4.65 (m, 1H), 4.23 (m, 3H), 3.92 (t, *J* = 7.5 Hz, 1H), 2.80 (s, 4H), 2.02 (m, 1H), 1.71 (m, 3H), 0.88 (m, 12H).

To the solution of Fmoc-L-Val-L-Leu-OSu in 60 mL of DMF was added dropwise a solution of *N*-(fluorenyl-9-methoxycarbonyl) L-Lys(*N*^ε-Boc) (2.18 g, 8.84 mmol) in 100 mL of cosolvent of THF/water (3:2) containing 2.3 mL of NMM at 0 °C. After addition, the reaction mixture became clear, and it was stirred for 48 h. It was filtered, and the filtrate was concentrated by removing THF in vacuo. The resulting mixture was diluted with 250 mL of EtOAc, washed with 10% aq citric acid, and dried (MgSO₄). It was filtered and dried by evaporation of the solvent in vacuo. The crude product was purified by column chromatography using silica gel as the stationary phase with a gradient eluent system (from DCM to 10% MeOH in DCM, *R*_f (10% MeOH in DCM) = 0.45), followed by crystallization from EtOAc to give a white powder (4.33 g, 72%). ¹H NMR (250 MHz, DMSO-*d*₆) δ (ppm): 8.05 (d, *J* = 5.0 Hz, 1H), 7.91 (t, *J* = 7.5 Hz, 3H), 7.73 (m, 2H), 7.42 (t, *J* = 5.0 Hz, 2H), 7.32 (t, *J* = 7.5 Hz, 2H), 6.79 (t, *J* = 5.0 Hz, 1H), 4.30 (m, 5H), 3.87 (t, *J* = 7.5 Hz, 1H), 2.86 (m, 2H), 1.99 (m, 1H), 1.65–1.20 (m, 19H), 0.83 (m, 12H). MS: calcd [M⁺] = 680, obsvd [M+1⁺] = 681.

Fmoc-L-Lys(Boc)-L-Leu-L-Val was synthesized starting from *N*-(fluorenyl-9-methoxycarbonyl) L-Lys (Boc) according to the above method in the route shown in Scheme 1.

Fmoc-L-Lys(Boc)-OSu. ¹H NMR (250 MHz, DMSO-*d*₆) δ (ppm): 8.11 (d, *J* = 7.5 Hz, 1H), 7.91 (d, *J* = 5.0 Hz, 2H), 7.70 (m, 2H), 7.42 (t, *J* = 7.5 Hz, 2H), 7.33 (t, *J* = 7.5 Hz, 2H), 6.79 (m, 1H), 4.33 (m, 4H), 2.91 (m, 2H), 2.82 (s, 4H), 1.79 (m, 2H), 1.37 (m, 13H).

Fmoc-L-Lys(Boc)-L-Leu. ¹H NMR (250 MHz, DMSO-*d*₆) δ (ppm): 8.06 (d, *J* = 7.5 Hz, 1H), 7.91 (d, *J* = 7.5 Hz, 2H), 7.74 (m, 2H), 7.42 (t, *J* = 7.5 Hz, 2H), 7.33 (t, *J* = 7.5 Hz, 2H), 6.78 (m, 1H), 4.24 (m, 4H), 3.99 (m, 1H), 2.89 (m, 2H), 1.66–1.20 (m, 18H), 0.86 (q, *J* = 7.5 Hz, 6H). MS: calcd [M⁺] = 581, obsvd [M+1⁺] = 582.

Fmoc-L-Lys(*N*^ε-Boc)-L-Leu-L-Val. *R*_f (10% MeOH in DCM) = 0.57; ¹H NMR (250 MHz, DMSO-*d*₆) δ (ppm): 7.97 (d, *J* = 7.5 Hz, 1H), 7.91 (d, *J* = 7.5 Hz, 2H), 7.88 (m, 1H), 7.78 (m, 2H), 7.50–7.30 (m, 4H), 6.77 (m, 1H), 4.39–4.11 (m, 5H), 3.99 (m, 1H), 2.89 (m, 2H), 2.02 (m, 1H), 1.70–1.20 (m, 19H), 0.86 (m, 12H). MS: calcd [M⁺] = 680, obsvd [M+1⁺] = 681.

Hydrogel Formation

A. Standard pH-adjusting method: Each Fmoc-tripeptide was added into a vial, followed by addition of 0.5 mL of

borate buffer with a concentration of 1% wt. The mixture was sonicated in an ultrasonic bath with shaking at 40–50 °C for 5–10 min. Upon cooling to room temperature, gelation was observed by the inverted vial method.

B. Each Fmoc-tripeptide (6.2 mg, 9.1 × 10⁻³ mmol) was first dispersed in 1.5 mL of water by sonication for 5 min, followed by careful addition of aq NaOH (1 M) to dissolve the Fmoc-tripeptide via vortexing so that a clear solution was obtained. To the basic peptide solution was added 15 mg of GdL¹¹ sonicated for 5 min at room temperature and then vortex mixed. Homogeneous hydrogels were formed in 15 min.

Congo Red Staining and Birefringence Monitored by Polarized Optical Microscopy.

Fresh Congo Red solution was made as follows: Sodium chloride was added in excess to an 80% ethanol solution, vortexed, and then filtered. Congo Red was added in excess to the saturated NaCl ethanol solution, and the resulting solution was vortexed and filtered.³² Congo Red solution was pipetted onto a glass microscope slide, and then the peptide gel was placed underneath the surface of the Congo Red solution and stained for approximately 1 min. After the excess Congo Red solution was removed by blotting, images of the sample placed between crossed polarizers were obtained with an Olympus CX-41 microscope.

Circular Dichroism (CD). The CD spectra were recorded using a Chirascan spectropolarimeter (Applied Photophysics, U.K.). Solutions of Fmoc-tripeptide in borate buffer (pH = 10) with a range of concentrations (0.1, 0.5, 1 wt %) were loaded into a 0.01 mm quartz cell (Hellma 0.01 mm quartz Suprasil). Spectra were obtained from 200 to 280 nm with a 0.5 nm step and 2.5 s collection time per step at 25 °C, taking four averages.

Fourier Transform Infrared (FTIR) and Raman Spectroscopy.

Spectra were recorded using a Nexus-FTIR spectrometer equipped with a DTGS detector and a multiple reflection attenuated total reflectance (ATR) system. Solutions of Fmoc-tripeptide in borate buffer (pH = 10) with a concentration of 1 wt % incubated for 16 h were sandwiched in ring spacers between two CaF₂ plate windows (spacer 0.006 mm). A spectrum for each sample was also measured for a film dried from a 1 wt % solution onto a CaF₂ plate. All spectra were scanned 128 times over the range of 4000–950 cm⁻¹.

Raman Spectroscopy. Raman spectra were recorded using a Renishaw inVia Raman microscope. The light source was a multiline laser, such that the experiments were performed using the λ = 785 nm edge. Experiments were made on stalks prepared by drying filaments of the peptide obtained from 2 wt % Fmoc-VLK(Boc) and 2 wt % Fmoc-KLV(Boc) gels in borate buffer. The stalks were focused by using a 20× magnification lens. Spectra were obtained in the interval 100–3000 cm⁻¹, using a 20 s collection time with 10% laser power and taking two averages.

Cryogenic-Transmission Electron Microscopy (Cryo-TEM).

Experiments were performed at Unilever Research, Colworth, Bedford, U.K. Sample preparation was carried out using a CryoPlunge 3 unit (Gatan Instruments) employing a double blot technique. The amount of 3 μ L of sample in borate buffer was pipetted onto a plasma etched (15 s) 400 mesh holey carbon grid (Agar Scientific) held in the plunge chamber at approximately 90% humidity. The samples were blotted, from both sides, for 0.5, 0.8, or 1.0 s depending on sample viscosity. The samples were then plunged into liquid ethane at a temperature of -170 °C. The grids were blotted to remove excess ethane and then transferred, under liquid nitrogen to the cryo-TEM specimen holder (Gatan 626 cryo holder) at -170 °C. Samples were examined using a Jeol 2100 transmission electron microscope operated at 200 kV and imaged using a Gatan Ultrascan 4000 camera, and images were captured using DigitalMicrograph software (Gatan).

Fiber X-ray Diffraction (XRD). X-ray diffraction was performed on the same stalks used for Raman experiments. The stalks were mounted (vertically) onto the four axis goniometer of a RAXIS IV++ X-ray diffractometer (Rigaku) equipped with a rotating anode generator. The XRD data were collected using a Saturn 992 CCD camera.

Small-Angle X-ray Scattering (SAXS). SAXS was performed on beamline I22 at Diamond Light Source, Harwell Science and Innovation Campus, U.K. The energy used was 12.4 keV with a 2.2 m camera length and beamstop in the middle of the RAPID 2D detector. The peptide gels were loaded into a liquid cell, placed between two mica windows, and then mounted directly into the sample position on the beamline. A total of six frames of 10s were collected. The same was also done for backgrounds.

Light Scattering. Static light scattering was performed using a custom built instrument described elsewhere.³⁰ Briefly, it comprises a He–Ne laser, an optics train, a sample contained in a Linkam CSS 450 shear cell, a diffuser plate, and a CCD camera to detect images. The sample was subjected to a range of shear rates; however, no significant orientation was observed, and so the two-dimensional patterns obtained were integrated to one-dimensional profiles of intensity versus scattering angle and hence wavenumber q (calibrated using a diffraction grating).

Rheology. The rheological properties of the systems were determined using a controlled stress AR-2000 rheometer from TA Instruments. A cone and plate geometry (20 mm diameter, 1° angle) was used for all samples. Frequency sweeps were performed in the angular frequency (ω) range 0.1–600 rad/s with the instrument in oscillatory mode at 25 °C. After an initial frequency sweep, another was carried out including a preshear (controlled stress mode) at 50 s⁻¹ for 2 min. Further frequency sweeps were then performed at regular intervals to investigate the recovery of the gel. To ensure that the moduli were independent of strain, preliminary strain sweeps were performed for each sample.

Results

a. Synthesis and Hydrogelation. Fmoc-VLK(Boc) and Fmoc-K(Boc)LV (Scheme 1) were synthesized by peptide bond formation via aminolysis of *N*-hydroxysuccinimidyl esters in aqueous/organic solvent.^{10,31} Since tripeptides Fmoc-VLK(Boc) and Fmoc-K(Boc)LV are soluble in basic media but insoluble in acid or neutral water, hydrogelation was initially investigated using basic solution. Fmoc-tripeptide (6.2 mg, 9.1 × 10⁻³ mmol) was first dispersed in 1.5 mL of water by sonication, followed by careful addition of aq NaOH (1 M) to dissolve the Fmoc-tripeptides with vortex mixing to obtain a clear solution. After 10 min, gelation took place, producing a transparent uniform gel with pH 12–13. In 1 h, it gradually became turbid, followed by collapse of the whole network. In contrast, a stable gel was achieved when borate buffer (pH = 10) was used as a solvent.³¹ However, the resulting gel was inhomogeneous with some denser regions in the network, probably due to the slower kinetics of mixing than that of gelation. Adams et al.¹¹ reported a new approach to prepare homogeneous hydrogels using GdL to control the acidic pH of the obtained hydrogels. With addition of GdL, we were able to prepare homogeneous transparent hydrogels based on tripeptides Fmoc-VLK(Boc) and Fmoc-K(Boc)LV, confirmed by the inverted vial method as shown in Figure 1. However, the focus of the remainder of this paper is on hydrogels in basic media, that is, in borate buffer.

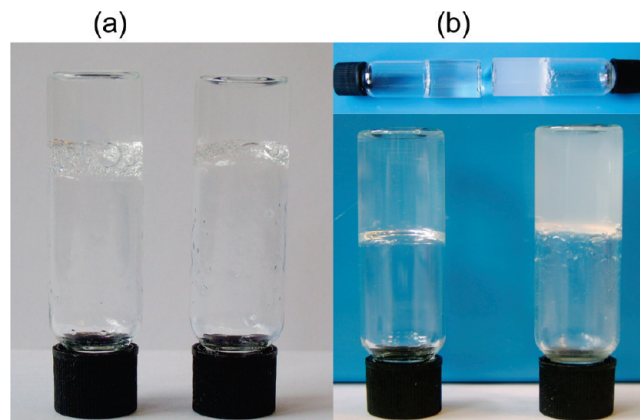


Figure 1. Self-supporting hydrogels of (left) Fmoc-VLK(Boc) and (right) Fmoc-K(Boc)LV in (a) borate buffer (pH = 10) and (b) GdL (pH ≈ 4).

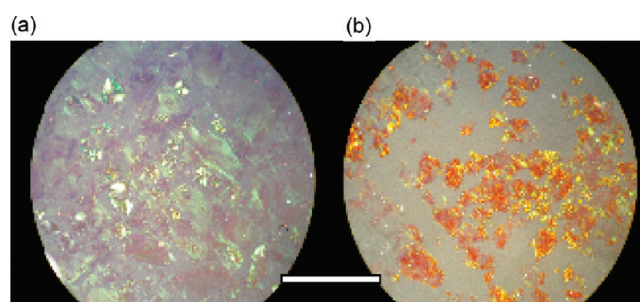


Figure 2. Polarized optical microscopy image of Fmoc-tripeptides stained with Congo Red: (a) Fmoc-VLK(Boc) and (b) Fmoc-K(Boc)LV. Scale bar indicates 1 mm.

b. Secondary Structure. Congo Red staining experiments showed strong green birefringence in the polarized optical microscope for Fmoc-VLK(Boc) over regions approximately 0.15 mm in size (Figure 2), suggesting amyloid formation. The yellow-green birefringence of sample Fmoc-KLV(BOC) is less pronounced, but there are clear areas with yellowish color, consistent with uptake of the dye.³¹ The uptake of Congo Red is usually considered to be a robust diagnostic of amyloid fibril formation, and this dye is taken up by fibrils and oligomers of many peptides and proteins forming cross- β structures.^{32,33} However, its mode of binding does depend on β -sheet structure,³³ and as discussed below the reduced binding to fibrils of Fmoc-KLV(Boc) may reflect differences in molecular packing within the fibrils.

The secondary structure of Fmoc-tripeptides was assessed using circular dichroism (CD) (Figure 3), measured for 1 wt % samples in pH 10 borate buffer. The peaks observed in two ranges of 210–220 nm and 240–260 nm showed features due to $n \rightarrow \pi^*$ and $\pi \rightarrow \pi^*$ transitions. Spectra with peaks in these regions have previously been reported for Fmoc-peptides such as Fmoc-tyrosine derivative.^{7,15} Fmoc-FF exhibits positive peaks in the CD spectrum at 200–210 and 260 nm, with a minimum at 218 nm, ascribed to β -sheet structure.³⁴ A β -sheet minimum at 215 nm is observed for Fmoc-K(Boc)LV (Figure 3) but not for Fmoc-VLK(Boc), for which a large positive maximum is observed at 220 nm. A detailed molecular interpretation of CD spectra for short peptides such as Fmoc-derivatives is still lacking and

(30) Castelletto, V.; Hamley, I. W. *Polym. Adv. Technol.* **2006**, *17*(3), 137–144.

(31) Teng, P. K.; Eisenberg, D. *Protein Eng., Des. Sel.* **2009**, *22*(8), 531–536.

(32) Lendel, C.; Bertoncini, C. W.; Cremades, N.; Waudby, C. A.; Vendruscolo, M.; Dobson, C. M.; Schenk, D.; Christodoulou, J.; Toth, G. *Biochemistry* **2009**, *48*(35), 8322–8334.

(33) Childers, W. S.; Mehta, A. K.; Lu, K.; Lynn, D. G. *J. Am. Chem. Soc.* **2009**, *131*(29), 10165–10172.

(34) Smith, A. M.; Williams, R. J.; Tang, C.; Coppo, P.; Collins, R. F.; Turner, M. L.; Saiani, A.; Ulijn, R. V. *Adv. Mater.* **2008**, *20*, 37–41.

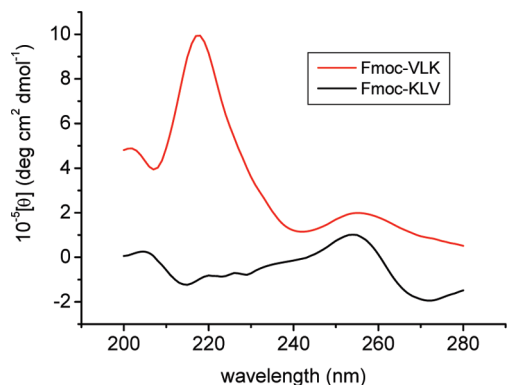


Figure 3. Circular dichroism spectra of Fmoc-VLK(Boc) and Fmoc-K(Boc)LV tripeptides (1 wt % in pH 10 borate buffer).

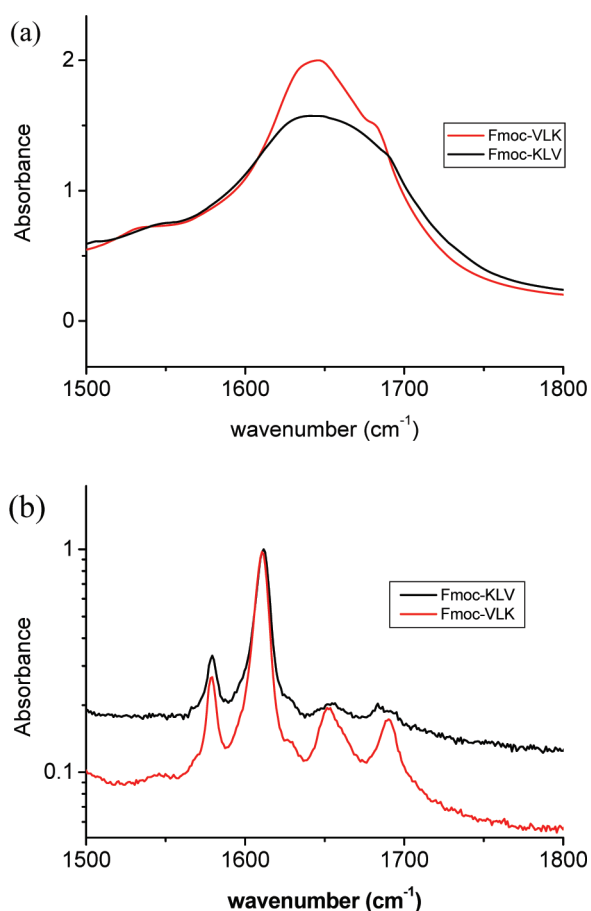


Figure 4. (a) FTIR spectra and (b) Raman spectra of the amide I region of Fmoc-VLK(Boc) and Fmoc-K(Boc)LV tripeptides (dried films from gels with a concentration of 1 wt % in pH 10 borate buffer).

prohibits further detailed interpretation. It can be noted that the spectrum obtained for Fmoc-K(Boc)LV is notably less intense (lower molar ellipticity) than that for Fmoc-VLK(Boc), pointing to lower chiral ordering in the former system. This may be related to the nature of the fibrils, which are quite straight for Fmoc-VLK(Boc) but highly branched for Fmoc-K(Boc)LV, as will be discussed shortly.

As the amide I band is sensitive to secondary structure, FTIR spectra of the two Fmoc tripeptides were recorded. Broad peaks centered at 1650 cm^{-1} were observed, with a shoulder around

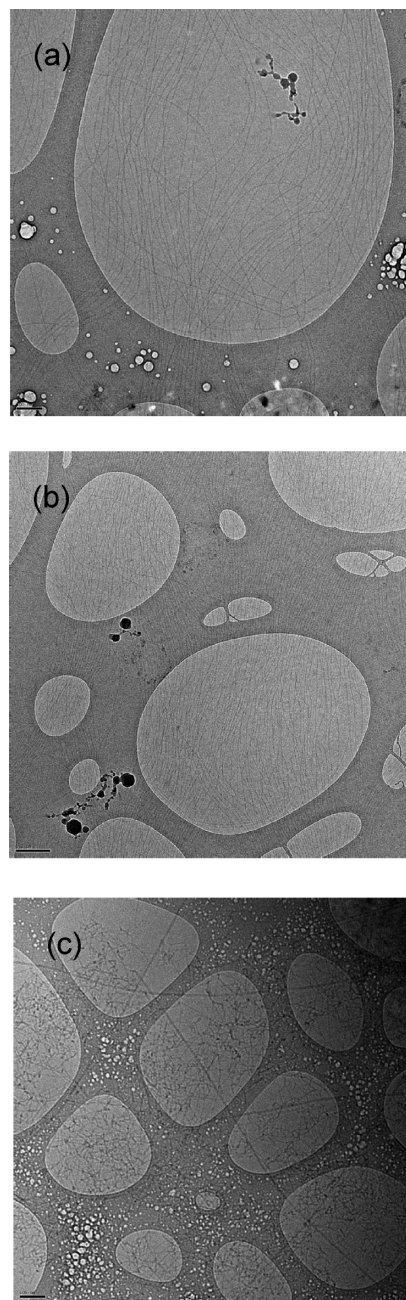


Figure 5. Cryo-TEM images of (a,b) Fmoc-VLK(Boc) and (c) Fmoc-K(Boc)LV. Scale bar in (a) represents 200 nm, and in (b,c) it represents 100 nm.

1685 cm^{-1} for the gels or dried gels (Figure 4a). The latter may be assigned to β -sheet structure. Deconvolution of the broad peaks was not attempted; their width suggests the presence of elements of β -sheet structure ($1625\text{--}1640\text{ cm}^{-1}$) and random coil ($1640\text{--}1650\text{ cm}^{-1}$) structures (the peptides are too short to form α -helices).^{22,34} Similar spectra were reported for Fmoc-TL and Fmoc-TF dipeptides.¹⁸ Raman spectroscopy can provide complementary information, and spectra were measured using stalks prepared from the two Fmoc-tripeptide gels (Figure 4b). Typically, a strong band at $1610\text{--}1625\text{ cm}^{-1}$ and a weak one at 1690 cm^{-1} were observed and associated with antiparallel β -sheet structure for both gels.²² A band centered at 1652 cm^{-1} (quite strong for Fmoc-VLK(Boc)) indicated the presence of non- β -sheet structure. As with circular dichroism, detailed molecular interpretation of FTIR spectra from short peptides is a current theoretical

challenge. We believe that interpretation of such spectra based on secondary structural elements from large proteins may not always be fully applicable.

c. Fibril Morphology and Superstructure: Electron Microscopy, Light Scattering, and X-ray Scattering. Cryo-TEM confirms that both Fmoc-VLK(Boc) and Fmoc-K(Boc)LV form fibrillar structures in 0.2 wt % borate buffer solution (Figure 5). The fibrils showed a high degree of alignment locally for the former sample, whereas for the latter sample mainly dense clusters of branched fibrils are observed, coexisting with a small number of quite straight fibrils, which are wider than the branched fibrils in the network clusters. The fibril diameter estimated from the cryo-TEM images is 8 nm for Fmoc-VLK(Boc) and 7 nm for the fine branched fibrils in Fmoc-K(Boc)LV, with 9 nm diameter larger straight fibrils. The dark blobs in the cryo-TEM images are ice crystals, and white bubbles are regions where evaporation has occurred due to exposure to the electron beam. These artefacts do not affect the imaging of the fibrils. Static light scattering confirmed a more branched structure for Fmoc-K(Boc)LV. A Kratky plot of the scattered intensity (Figure 6) shows a more pronounced maximum for this peptide, consistent with a more branched structure.^{22,35}

SAXS also confirmed that both samples self-assemble into fibrils in pH 10 borate buffer solution. Figure 7 shows intensity profiles with fits for the lower concentration data (1 wt %; this is higher than cryo-TEM or CD data in order to achieve good scattering data, i.e. sufficient signal/noise ratio) for Fmoc-VLK(Boc) to a model form factor for a polydisperse uniform cylinder.³⁶ The fit indicates a diameter $D = 4.2 \pm 0.3$ nm, which is lower than the fibril diameter obtained from cryo-TEM (8 nm); however, a hydrated boundary layer may not be detectable by SAXS. The data for Fmoc-K(Boc)LV could not be fitted to a simple polydisperse cylinder form factor (the slope of the intensity profile at low q is approximately $q^{-2.5}$, whereas q^{-1} is expected for cylinders). Instead, we were able to fit the data to the structure factor for a mass fractal object, with an exponential cutoff, using the freely available software SASfit.³⁷ This structure factor captures the branched nature of the fibrillar network. The corresponding structure factor intensity is given by³⁸

$$I(q) = \frac{\sin[(D-1) \tan^{-1}(q\xi)]}{(D-1)q\xi(1+q^2\xi^2)^{(D-1)/2}} \quad (1)$$

Here, D is the fractal dimension, $\xi^2 = 2R_g^2/D(D+1)$, and R_g is the radius of gyration of the fractal aggregate. From the fit, we obtained $D = 2.5$ and $R_g = 10.4$ nm for the Fmoc-K(Boc)LV data (1 wt %).

The 2 wt % gel of Fmoc-K(Boc)LV shows a broad structure factor peak, centered at $q^* = 0.071 \text{ \AA}^{-1}$, corresponding to a structure with a domain size $d = 89 \text{ \AA}$. This is in very close agreement with the fibril diameter obtained from the cryo-TEM image (Figure 5c) and suggests close-packing of the fibrils. The alignment of fibrils observed by cryo-TEM for gels formed by Fmoc-VLK(Boc) is also reflected in anisotropic SAXS patterns; see Figure 8 for example. The anisotropy results from spontaneous macroscopic alignment of the sample when poured into the

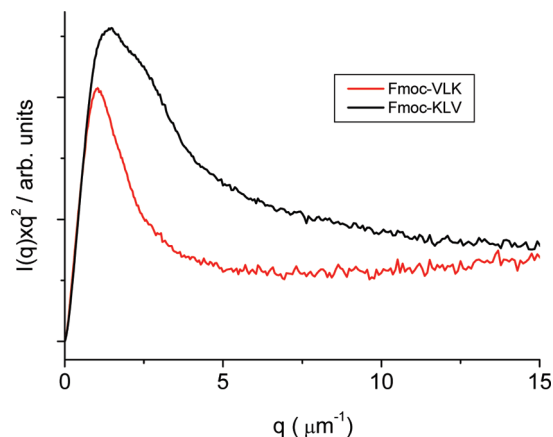


Figure 6. Static light scattering data presented in Kratky-plot format.

cell used for SAXS experiments. In contrast, orientation was not observed in SAXS patterns for Fmoc-K(Boc)LV.

Fiber X-ray diffraction was performed on dried stalks to obtain information on molecular packing. Figure 9 compares XRD patterns for the two compounds. Some features are common to the data for both systems; in particular, a series of reflections can be ascribed to the cross- β pattern observed for β -sheet fibrils.³⁹ At higher angle, sharper reflections are observed that are ascribed to the borate buffer (a separate XRD pattern was obtained on a dried borate buffer solution, data not shown, strong reflections listed in Table 1).

The fiber diffraction pattern for Fmoc-VLK(Boc) shows a high degree of alignment. There are meridional 4.7 \AA reflections and series of equatorial reflections, of which the strongest corresponds to a spacing of 21.5 \AA . The high degree of alignment of the diffraction pattern reflects the local orientation of fibrils observed by cryo-TEM (Figure 5a,b) and the macroscopic alignment in the SAXS pattern (Figure 8a). Much sharper reflections are observed at higher angle, and since the peak width is different from the cross- β pattern peaks, these are associated with features not related to β -sheets. We believe they result from the buffer. All reflections are listed in Table 1. The reflections observed for Fmoc-VLK(Boc) may be indexed to an orthorhombic unit cell.

The X-ray diffraction pattern for Fmoc-K(Boc)LV (Figure 9b) shows very little orientation, consistent with the observed entangled nature of the fibrils observed for this sample (Figure 5c). Peaks at low angle (Table 1) can be assigned to an unoriented cross- β structure. A larger number of strong reflections are observed at low angle than those for Fmoc-VLK(Boc). Since these peaks are associated with stacking of β -sheets, this may indicate more ordered β -sheet stacks within the Fmoc-K(Boc)LV fibrils. The d -spacing at 4.88 \AA is somewhat larger than that observed for Fmoc-VLK(Boc) for which the corresponding strong meridional reflection is observed at 4.74 \AA ; however, it is within the range observed for β -sheets.⁴⁰ The difference in this interstrand spacing may reflect differences in molecular conformation or packing motif within the sheets. For Fmoc-K(Boc)LV, a series of sharp reflections are again observed at higher angle, with the principal one being at 3.2 \AA , as for Fmoc-VLK(Boc), which is ascribed to the buffer (Table 1). A slightly larger spacing of 3.4 \AA was ascribed to phosphate buffer in XRD data presented for Fmoc-LLL, while an Fmoc stacking distance was observed

(35) Pallitto, M. M.; Ghanta, J.; Heinzelman, P.; Kiessling, L. L.; Murphy, R. M. *Biochemistry* **1999**, *38*, 3570–3578.

(36) Krysmann, M. J.; Castelletto, V.; Hamley, I. W. *Soft Matter* **2007**, *3*, 1401–1406.

(37) <http://kur.web.psi.ch/sans1/SANSSoft/sasfit.html> (2009).

(38) Sorensen, C. M.; Wang, G. M. *Phys. Rev. E* **1999**, *60*(6), 7143–7148.

(39) Hamley, I. W. *Angew. Chem., Int. Ed.* **2007**, *46*, 8128–8147.

(40) Nelson, R.; Sawaya, M. R.; Balbirnie, M.; Madsen, A. O.; Riekel, C.; Grothe, R.; Eisenberg, D. *Nature (London)* **2005**, *435*, 773–778.

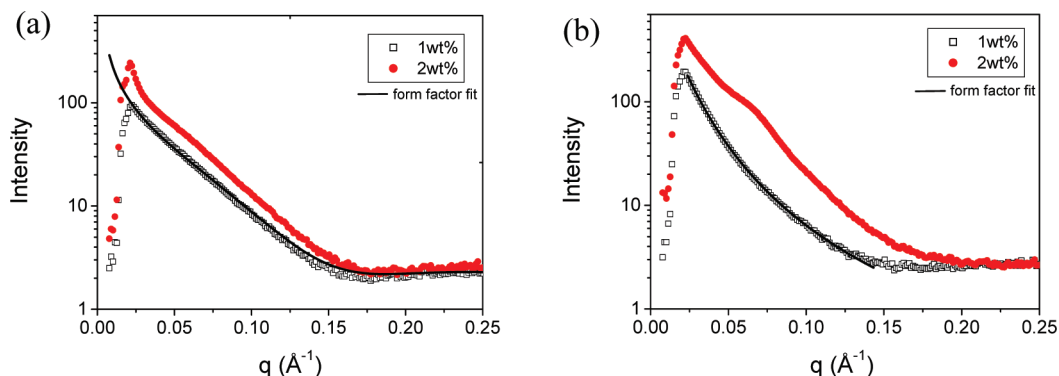


Figure 7. SAXS profiles (obtained by radial integration of 2-D patterns) for (a) Fmoc-VLK(Boc) and (b) Fmoc-K(Boc)LV. Fitted intensity profiles are included, as discussed in the text.

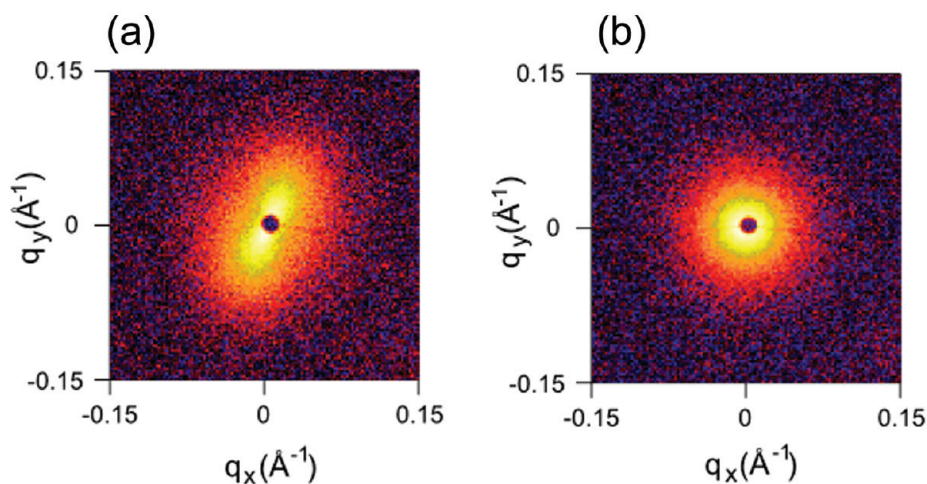


Figure 8. SAXS patterns for 1 wt % solutions of (a) Fmoc-VLK(Boc) and (b) Fmoc-K(Boc)LV.

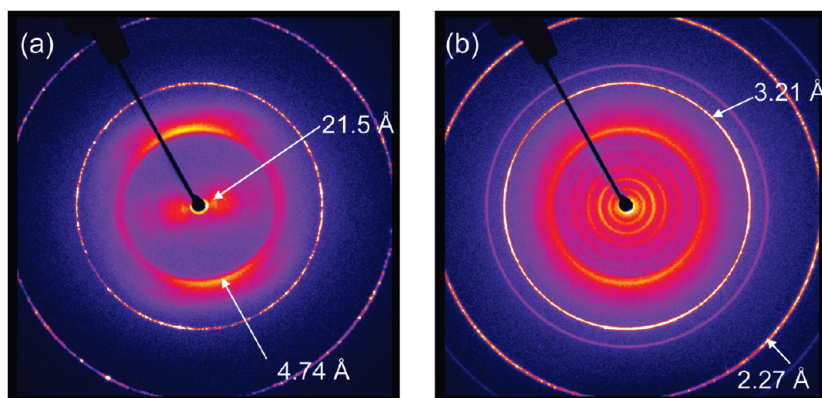


Figure 9. Fiber X-ray diffraction patterns for (a) Fmoc-VLK(Boc) and (b) Fmoc-K(Boc)LV.

at 3.8 Å.⁴¹ It is interesting that a strong peak at around this distance is not observed for either of our samples, suggesting less regular packing of the Fmoc groups, possibly due to greater conformational flexibility of the attached tripeptide.

d. Gel Rheology. Oscillatory shear rheometry was used to probe the dynamic mechanical properties of hydrogels formed by 1 and 2 wt % gels of Fmoc-VLK(Boc) and Fmoc-K(Boc)LV.

Figure 10 shows frequency sweep data. The two peptides exhibit distinct behavior. Fmoc-VLK(Boc) forms a weak gel at 1 wt %, characterized by a low value of $G' \sim 100$ Pa at low frequency. The upturn in moduli at high frequency may be due to a thickening instability. The 2 wt % gel of Fmoc-VLK(Boc) has a higher modulus $G' > 4000$ Pa. A pronounced shear thinning is observed after preshearing. Partial recovery of the moduli is observed after several hours. Incomplete recovery is probably due to shear alignment, as observed by SAXS (Figure 8a).

Fmoc-K(Boc)LV forms stiff hydrogels at 1 and 2 wt % (Figure 10c,d), with a weakly frequency-dependent $G' > 10^5$ Pa.

(41) Xu, H.; Das, A. K.; Horie, M.; Shaik, M. S.; Smith, A. M.; Luo, Y.; Lu, X.; Collins, R.; Liem, S. Y.; Song, A.; Popelier, P. L. A.; Turner, M. L.; Xiao, P.; Kinloch, I. A.; Ulijn, R. V. *Nanoscale* **2010**, submitted.

Table 1. Spacings (in Å) from X-ray Diffraction Patterns^a

Fmoc-VLK(Boc)	Fmoc-KLV(Boc)	borate buffer ^b
21.4 (e)	21.1	
17.3 (e)		
13.8 (e)	13.4	
9.90 (m)	9.46	
	8.33	
6.85 (e)	6.76	
	5.85	
4.74 (m)	4.88	
3.32 (e)	4.26	
3.20 (s)	3.22 (s)	3.26 (s)
	2.88 (s)	2.79 (s)
2.27 (s)	2.27 (s)	2.28 (s)

^a Key: e, equatorial; m, meridional; s, sharp. ^b Strong peaks only.

Shear thinning is again observed after application of stress for 2 min; however, recovery is largely complete after 2 h (at high frequency). This correlates to the fact that orientation of the gels is not observed by SAXS.

Summary and Discussion

It is remarkable that a small sequence difference, that is, exchange of two residues, leads to dramatically different properties of Fmoc-VLK(Boc) and Fmoc-K(Boc)LV. A detailed molecular level understanding of how differences in packing motif influence self-assembly and ultimately macroscopic properties such as gelation (and gel modulus) and flow alignment is still lacking. Molecular modeling of isolated molecules suggested a more compact conformation for Fmoc-K(Boc)LV with the lysine side chain and Fmoc units forming two “arms” within the molecule. Interaction between Fmoc and Boc-protected lysine in Fmoc-K(Boc)LV may favor bending of the β -sheets and hence less straight fibrils compared to Fmoc-VLK(Boc). This interaction may be stabilized in part by hydrophobic interactions but also by cation- π interactions,⁴² since the amide nitrogen has a positive charge. The CD data show lower chiral ordering of Fmoc-K(Boc)LV compared to Fmoc-VLK(Boc). Fuller modeling would require extensive simulation beyond the single molecule level, considering different possible packing motifs and so on. This is planned for future work.

Other recent work on other self-assembling peptides has shown that subtle sequence differences can substantially impact properties such as gel properties. The hydrogels of Fmoc-VLK(Boc) have a modulus $G' > 10^4$ Pa. This is actually rather high compared to previously reported values for Fmoc-peptide hydrogels and other self-assembling peptide gels. Fmoc-FF hydrogels have $G' < 3$ Pa (depending on frequency).⁴³ The authors comment that higher values observed previously in their group⁶ might be due to kinetically trapped aggregates which reinforce the mechanical properties of the gels. However, a modulus $> 10^4$ Pa for a 0.5 wt % sample in water was reported in an earlier independent study of Fmoc-FF self-assembly and hydrogelation.¹⁰ A modulus approaching $G' = 10^4$ Pa has been reported for an Fmoc-tyrosine phosphatase hydrogel,^{7,15} and naphthalene-dipeptide hydrogels have been reported with similar moduli.⁸ The influence of sequence design within β -hairpin peptides (each strand comprising a similar hydrophobic/polar alternating sequence with a V^PPPT tetrapeptide β -turn) on hydrogel properties has also been probed; in particular, substitution of a single lysine by other residues changes the total charge on the peptide and enables more

rapid self-assembly.^{44–46} Substitution of one lysine with one glutamic acid lead to more rapid self-assembly due to reduced net charge per peptide, and a more branched hydrogel, as characterized by small-angle neutron scattering.⁴⁶ The modulus reported for this type of β -hairpin hydrogel ranges up to $G' = 1000–4000$ Pa depending on the peptide, its concentration, and buffer.^{45,47–49} In borate buffer under similar conditions to those of our Fmoc-tripeptide hydrogels, a modulus $G' = 1000$ Pa was reported.⁴⁸ The modulus of this type of peptide hydrogel can also be tuned by addition of salt which causes electrostatic screening.⁴⁹ Saiani and co-workers investigated the influence of sequence design on self-assembly and hydrogelation for octapeptides comprising alternating hydrophobic and charged residues, and hydrogels were observed for FEFKFEFK and FEFKFEFK.⁵⁰ In the case of our two peptides, the overall charge is the same; therefore, in contrast to previous studies such as that on β -hairpin peptides mentioned above,⁴⁶ this cannot explain the difference in branching in the fibrillar peptide networks. It is likely that the distribution of charge is different due to conformational differences, in particular due to the cation- π interaction between adjacent Fmoc and K residues in Fmoc-K(Boc)LV.

To our knowledge, flow-induced orientational ordering of Fmoc-peptide hydrogels has not previously been noted. We checked birefringence of the gel formed by Fmoc-VLK(Boc), and none was observed. This means that the alignment of fibrils observed by cryo-TEM and SAXS is only local and there is no long-range nematic order leading to birefringence. Nematic ordering within gels has been reported for a de novo designed peptide fragment.⁵¹ Nematic ordering within fluid peptide solutions has also been reported for several natural and synthetic peptides, as well as poly(ethylene glycol)/peptide conjugates as summarized elsewhere.⁵² Observation of nematic ordering requires sufficient fibril anisotropy, quantified in terms of diameter/length at a given concentration, approximately according to the Onsager criterion.⁵³ It is an interesting question as to the conditions which favor viscoelastic nematic fluid ordering as opposed to nematic gel formation.⁵¹ Entanglements or branching effects might predominate, depending on fibril persistence length.

The self-assembly motif may be compared to previous work on Fmoc-tripeptides. In contrast to Fmoc-LLL,⁴¹ cryo-TEM reveals that Fmoc-VLK(Boc) and Fmoc-K(Boc)LV form fibrils and not nanotubes. Fmoc-K(Boc)LV is intriguing in that while it does not take up Congo Red stain as readily as Fmoc-VLK(Boc), it does show features in FTIR and Raman spectra associated with β -sheet structure. In addition, the fiber X-ray diffraction pattern reveals an interstrand spacing somewhat larger than usually

(44) Rajagopal, K.; Lamm, M. S.; Haines-Butterick, L. A.; Pochan, D. J.; Schneider, J. P. *Biomacromolecules* **2009**, *10*(9), 2619–2625.

(45) Hule, R. A.; Nagarkar, R. P.; Altunbas, A.; Ramay, H. R.; Branco, M. C.; Schneider, J. P.; Pochan, D. J. *Faraday Discuss.* **2008**, *139*, 251–264.

(46) Branco, M. C.; Nettesheim, F.; Pochan, D. J.; Schneider, J. P.; Wagner, N. J. *Biomacromolecules* **2009**, *10*(6), 1374–1380.

(47) Schneider, J. P.; Pochan, D. J.; Ozbas, B.; Rajogopal, K.; Pakstis, L.; Kretsinger, J. J. *Am. Chem. Soc.* **2002**, *124*, 15030–15037.

(48) Pochan, D. J.; Schneider, J. P.; Kretsinger, J.; Ozbas, B.; Rajogopal, K.; Haines, L. J. *Am. Chem. Soc.* **2003**, *125*, 11802–11803.

(49) Ozbas, B.; Kretsinger, J.; Rajogopal, K.; Schneider, J. P.; Pochan, D. J. *Macromolecules* **2004**, *37*, 7331–7337.

(50) Saiani, A.; Mohammed, A.; Frielinghaus, H.; Collins, R.; Hodson, N.; Kieley, C. M.; Sherratt, M. J.; Miller, A. F. *Soft Matter* **2009**, *5*(1), 193–202.

(51) Aggeli, A.; Nyrkova, I. A.; Bell, M.; Harding, R.; Carrick, L.; McLeish, T. C. B.; Semenov, A. N.; Boden, N. *Proc. Natl. Acad. Sci. U.S.A.* **2001**, *98*(21), 11857–11862.

(52) Hamley, I. W.; Castelletto, V.; Moulton, C. M.; Myatt, D.; Siligardi, G.; Oliveira, C. L. P.; Pedersen, J. S.; Gavish, I.; Danino, D. *Macromol. Biosci.* **2010**, *10*, 40–48.

(53) Hamley, I. W. *Introduction to Soft Matter. Revised Edition*; Wiley: Chichester, 2007.

(42) Ma, J. C.; Dougherty, D. A. *Chem. Rev.* **1997**, *97*, 1303–1324.

(43) Tang, C.; Smith, A. M.; Collins, R. F.; Ulijn, R. V.; Saiani, A. *Langmuir* **2009**, *25*(16), 9447–9453.

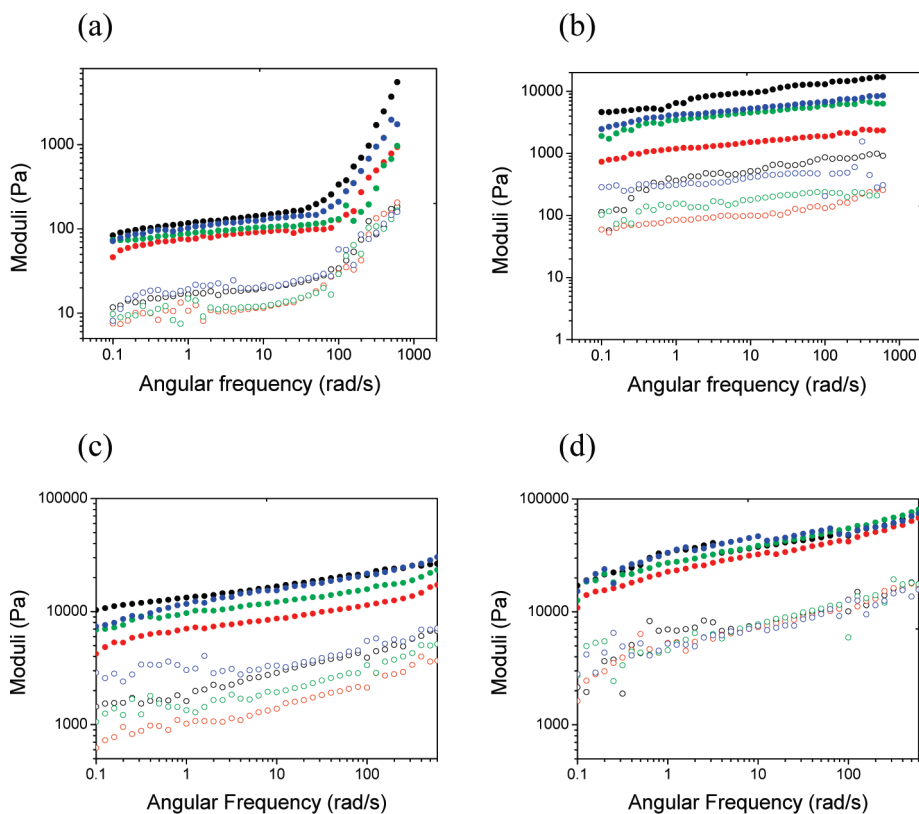


Figure 10. Dynamic shear moduli as a function of frequency: solid symbols, G' ; open symbols, G'' . Black, as mounted; red, preshear of 50 s^{-1} for 2 min; green, 1 h after preshear; blue, 2 h after preshear. (a) 1 wt % Fmoc-VLK(Boc), (b) 2 wt % Fmoc-VLK(Boc), (c) 1 wt % Fmoc-KLV(Boc), and (d) 2 wt % Fmoc-KLV(Boc).

observed. This points possibly to a distinct β -sheet packing structure instead of the conventional one, as exhibited, for example, by Fmoc-VLK(Boc).

In summary, our results show that sequence design, in particular use of (N^E -Boc)K, offers the ability to control intermolecular interactions and hence ultimate hydrogel properties of simple model tripeptides via differences in fibril self-assembly properties. The tunable gel modulus may be useful in applications such as regenerative medicine, as it has previously been shown that Fmoc-peptides can serve as three-dimensional scaffolds for cell culture^{5,6} among other applications as functional nanomaterials for biology

and medicine.¹ The aligned fibrillar structure of Fmoc-VLK(Boc), and flow alignment properties, may be useful, for instance, where an aligned medium is needed, for example, in controlling stem cell morphology.⁵⁴

Acknowledgment. This work was supported by EPSRC Grants EP/F048114/1 and EP/G026203/1. We are grateful to Steve Fuzeland and Derek Atkins (Unilever, Colworth, U.K.) for the cryo-TEM experiments.

(54) Mata, A.; Hsu, L.; Capito, R.; Aparicio, C.; Henrikson, K.; Stupp, S. I. *Soft Matter* **2009**, *5*, 1228–1236.